Antivascular Therapy for Orthotopic Human Ovarian Carcinoma through Blockade of the Vascular Endothelial Growth Factor and Epidermal Growth Factor Receptors

Premal H. Thaker,[1,2] Sertac Yazici,[1] Monique B. Nilsson,[1] Kenji Yokoi,[1] Rachel Z. Tsan,[1] Junqin He,[1] Sun-Jin Kim,[1] Isaiah J. Fidler,[1] and Anil K. Sood[1,2]

Abstract

Purpose: We determined whether the administration of the tyrosine kinase inhibitor, AEE788, which targets the epidermal growth factor receptor and the vascular endothelial growth factor receptor, alone or in combination with paclitaxel, can inhibit progressive growth of human ovarian carcinoma in the peritoneal cavity of female nude mice.

Experimental Design: Western blot analysis and immunohistochemical analysis identified the optimal dose and schedule of AEE788 therapy. In several different experiments, paclitaxel-sensitive and paclitaxel-resistant human ovarian carcinoma cells were injected into the peritoneal cavity of nude mice. Seven days later, treatment with saline (control), AEE788 alone, paclitaxel alone, or a combination of AEE788 and paclitaxel began and continued for 45 days when the mice were necropsied. In independent survival experiments, the mice were necropsied when they became moribund.

Results: Oral administration of AEE788 inhibited phosphorylation of the epidermal growth factor receptor and vascular endothelial growth factor receptor for up to 48 hours. Treatment with AEE788 plus paclitaxel significantly reduced tumor weight and increased survival of mice implanted with paclitaxel-sensitive cell lines compared with control mice or mice treated with AEE788 alone or paclitaxel alone. In mice implanted with paclitaxel-resistant cells, the combination therapy also significantly reduced tumor weight but did not prolong survival. The combination therapy induced apoptosis of both tumor cells and tumor-associated endothelial cells.

Conclusions: The administration of AEE788 and paclitaxel inhibits the progression of human ovarian carcinoma in the peritoneal cavity of female nude mice, in part, by inducing apoptosis of tumor-associated endothelial cells.

Ovarian carcinoma is the leading cause of death from gynecologic cancer (1). Despite initial tumor response rates of 80% to frontline taxane- and platinum-based chemotherapy and surgical debulking (2, 3), most women with advanced ovarian carcinoma will ultimately develop drug-resistant disease (4, 5). The use of second-line chemotherapeutic agents, such as doxorubicin, topotecan, gemcitabine, tamoxifen, and vinorelbine, can lead to a response rate of ~15% to 25% (6). Clearly, the development of better therapeutic strategies requires a better understanding of the biology of ovarian carcinoma.

Authors' Affiliations: Departments of [1]Cancer Biology and [2]Gynecologic Oncology, University of Texas M.D. Anderson Cancer Center, Houston, Texas

Received 10/7/04; revised 3/18/05; accepted 4/14/05.

Grant support: Cancer Center support grant CA16672 and Specialized Programs of Research Excellence in Ovarian Cancer grant CA93639 from the National Cancer Institute, NIH.

The costs of publication of this article were defrayed in part by the payment of page charges. This article must therefore be hereby marked *advertisement* in accordance with 18 U.S.C. Section 1734 solely to indicate this fact.

Requests for reprints: Anil K. Sood, Departments of Gynecologic Oncology and Cancer Biology, University of Texas M.D. Anderson Cancer Center, Unit 1362, P.O. Box 301439, Houston, TX 77230-1439. Phone: 713-745-5266; Fax: 713-792-7586; E-mail: asood@mdanderson.org.

The growth and metastasis of neoplasms, including ovarian carcinoma, depend on the formation of adequate vasculature (i.e., angiogenesis; ref. 7). Vascular endothelial growth factor (VEGF) is one of many proangiogenic factors whose receptors include VEGFR-1 (Flt-1) and VEGFR-2 (KDR/Flk-1; ref. 8). Hypoxia, an important stimulus for VEGF production by both normal and tumor cells, can stimulate vascular permeability and angiogenesis (9). The expression of VEGF is substantially increased in solid cancers, leading to greater microvascular density and a poor prognosis (10). Several published reports implicate VEGF and VEGFR in the growth of ovarian carcinoma. Expression of VEGF, VEGFR-1, and VEGFR-2 was noted in malignant mucinous and serous tumors and in some borderline tumors, but not in benign tumors (11). In early-stage ovarian cancer, overexpression of VEGF has been associated with a shortened disease-free survival (12). Additionally, elevated preoperative VEGF levels have been shown to be an independent prognostic factor for patients with ovarian carcinoma (13). VEGF levels are elevated in ascites, and inhibitors of VEGF activity have been shown to reduce the formation of malignant ascites and tumor growth in human ovarian carcinoma xenograft models (14).

The epidermal growth factor (EGF) and its receptor (EGFR) play a critical role in the progression of ovarian carcinoma. EGF stimulates proliferation of both normal ovarian epithelial cells

and ovarian cancer cells via autocrine and paracrine mechanisms (15, 16). Elevated levels of the EGFR have been detected in ovarian tumors, in ascites, and in the urine of ovarian cancer patients (17, 18). EGF stimulates the production of matrix metalloproteinase-9, which is commonly elevated in samples of invasive epithelial ovarian carcinoma from patients, leading to invasion (19, 20). The EGFR is reported to be present in 33% to 75% of ovarian cancers (15, 21). High expression levels of EGFR and ErbB2 correlate with poor survival (17, 21). Expression of EGFR in ovarian cancer patients also correlates with decreased expression of α_5-integrin subunit and matrix metalloproteinase-9 activity, which are critical for invasion (22). Collectively, these data show that VEGF, VEGFR, EGF, and EGFR have critical roles in the progressive growth of ovarian carcinoma.

AEE788 (molecular weight, 440.6 kDa) is a recently described specific kinase inhibitor targeting both EGFR and VEGFR. It belongs to the class of the 7*H*-pyrrolo[2,3-*d*] pyrimidines (23). In this study, we evaluated whether blockade of the VEGFR and EGFR activation by AEE788 can decrease the progressive growth of human ovarian cancer cells implanted into the peritoneal cavity of nude mice. We show that oral administration of AEE788 thrice per week combined with once weekly i.p. injection of paclitaxel induced apoptosis of tumor cells and tumor-associated endothelial cells and significantly increased survival in these mice.

Materials and Methods

Ovarian cancer cell lines, organ-specific endothelial cells, and culture conditions. For these studies, we used highly metastatic human ovarian cancer cell lines Hey A8, SKOV3ip1, and the taxane-resistant cell line Hey A8-MDR. The derivation and sources of the cell lines have been previously reported (24–27). SKOV3ip1 and Hey A8 cells were grown as monolayer cultures in complete MEM (Life Technologies, Inc., Grand Island, NY) supplemented with 10% fetal bovine serum, vitamins, sodium pyruvate, L-glutamine, nonessential amino acids (Life Technologies), and penicillin-streptomycin (Flow Laboratories, Rockville, MD). Hey A8 paclitaxel-resistant cells were grown in complete MEM containing 300 ng/mL paclitaxel (Taxol, Bristol-Myers Squibb, Co., Princeton, NJ). The tumor cells were tested and found to be free of *Mycoplasma* and pathogenic murine viruses, as previously reported (27).

Organ-specific endothelial cell lines from the ovary and mesentery were derived from female mice homozygous for a temperature-sensitive SV40 large T antigen (ImmortoMice; CBA/ca × C57Bl/10 hybrid; Charles River Laboratories, Wilmington, MA; ref. 28). The endothelial cells were maintained in monolayer cultures in DMEM supplemented with 10% fetal bovine serum, vitamins, sodium pyruvate, L-glutamine, nonessential amino acids (Life Technologies), and penicillin-streptomycin (Flow Laboratories). Monolayers were initially incubated at 33°C and then changed to a 37°C incubator to become terminally differentiated. The endothelial cells were free of *Mycoplasma* and pathogenic murine viruses (assayed by Science Applications International Corporation).

Reagents. Primary antibodies were purchased from the following manufacturers: rabbit anti–phosphorylated (p)-VEGFR-2/3 (Flk-1; Oncogene, Boston, MA); rabbit anti-human, mouse, rat VEGFR (C1158; Santa Cruz Biotechnology, Santa Cruz, CA); rabbit anti-human p-EGFR (Tyr^{1173}; Biosource, Camarillo, CA); rabbit anti-human EGFR for paraffin samples (Santa Cruz Biotechnology); rabbit anti-human EGFR for frozen samples (Zymed, San Francisco, CA); rat anti-mouse CD31 (BD PharMingen, San Diego, CA); mouse anti–proliferating cell nuclear antigen (PCNA) clone PC 10 (Dako, A/S, Copenhagen, Denmark); and rabbit anti-mouse, human, rat phosphorylated-Akt (p-Akt; Cell Signaling, Beverly, MA). The following secondary antibodies were used for colorimetric immunohistochemistry: peroxidase-conjugated goat anti-rabbit IgG; F(ab′)2 (Jackson ImmunoResearch Laboratories, Inc., West Grove, PA); biotinylated goat anti-rabbit (Biocare Medical, Walnut Creek, CA); streptavidin horseradish peroxidase (DAKO); rat anti-mouse IgG2a horseradish peroxidase (Serotec, Harlan Bioproducts for Science, Inc., Indianapolis, IN); and goat anti-rat horseradish peroxidase (Jackson ImmunoResearch Laboratories). The following fluorescent secondary antibodies were used: goat anti-rabbit Alexa 488 and goat anti-rat Alexa 594 (Molecular Probes, Inc., Eugene, OR). Terminal deoxynucleotidyl transferase-mediated nick end labeling (TUNEL) staining was done using a commercial apoptosis detection kit (Promega, Madison, WI) with modifications. Other reagents include Hoechst 3342 dye (Polysciences, Inc., Warrington, PA), stable 3,3′-diaminobenzidine (Research Genetics, Huntsville, AL), Gill's hematoxylin (Sigma-Aldrich Corp, St. Louis, MO), cold water fish skin gelatin 40% (Electron Microscopy Sciences, Fort Washington, PA), and propyl gallate (ACROS Organics, Morris Plains, NJ).

AEE788 was generously provided by Novartis Pharma, AG (Basel, Switzerland). For *in vitro* administration, AEE788 was dissolved in DMSO (Sigma-Aldrich) to a concentration of 20 mmol/L and further diluted to the appropriate final concentration in RPMI 1640 with 10% fetal bovine serum. DMSO in the final solution did not exceed 0.1% v/v. For *in vivo* administration (oral), AEE788 was dissolved in *N*-methylpyrrolidone and polyethylene glycol 300 1:9 (v/v). The AEE788 solution was prepared just before it was administered to the mice. Paclitaxel (Mead Johnson, Princeton, NJ) was diluted 1:6 in PBS for i.p. injections.

Western blot analysis. Cultures of Hey A8 and SKOV3ip1, mesenteric endothelial cells, and ovarian endothelial cells were washed twice with ice-cold PBS, and the cells were scraped into PBS containing 5 mmol/L EDTA and 1 mmol/L sodium orthovanadate, and centrifuged. The resulting pellet was resuspended in protein lysis buffer [20 mmol/L Tris-HCl (pH 8.0), 137 mmol/L sodium chloride, 10% glycerol, 2 mmol/L EDTA, 1 mmol/L phenylmethylsulfonyl fluoride, 1% aprotinin, 20 μmol/L leupeptin, and 0.15 unit/mL aprotinin]. The protein content of the samples was quantified spectrophotometrically. Aliquots of 60 μg protein were subjected to electrophoresis on 10% polyacrylamide gels. The protein was then transferred to a nitrocellulose membrane (Millipore, Bedford, MA) by electrotransfer. Following blocking with 3% bovine serum albumin in 0.5% Tween 20 in TBS [20 mmol/L Tris-HCl (pH 7.5), 150 mmol/L NaCl, and 0.1% Tween 20], the membrane was probed with a primary antibody [1:500 dilution of rabbit anti-VEGFR antibody (Santa Cruz Biotechnology); 1:20,000 dilution of rabbit anti-p-VEGFR antibody (Oncogene); 1:1,000 dilution of rabbit anti-EGFR antibody (Upstate Biotechnology, Lake Placid, NY); and 1:1,000 dilution of rabbit anti-p-EGFR antibody (Cell Signaling)]. The membranes were then washed and treated with a secondary antibody conjugated to horseradish peroxidase (goat anti-rabbit at a 1:2,000 dilution, Jackson ImmunoResearch Laboratories). Protein bands were visualized using a commercially available chemiluminescence kit (Amersham Biosciences, Piscataway, NJ).

To determine the dose of AEE788 required to inhibit phosphorylation of the VEGFR and EGFR, 3×10^6 SKOV3ip1 and Hey A8 cells were plated. Twenty-four hours later, the medium was removed and the cells were washed twice with PBS and incubated for 2 hours in serum-free medium with different concentrations of AEE788 in the presence or absence of 40 ng/mL recombinant human EGF (Santa Cruz Biotechnology). The cells were then harvested and processed as described above.

Animals. Female athymic nude mice (NCr-*nu*) were purchased from the Animal Production Area of the National Cancer Institute-Frederick Cancer Research and Development Center (Frederick, MD). The mice were housed and maintained under specific pathogen-free conditions in facilities approved by the American Association for Accreditation of Laboratory Animal Care in accordance with current regulations and standards of the U.S. Department of Agriculture, U.S. Department of Health and Human Services, and the NIH. The mice were used according to institutional guidelines when they were 8 to 12 weeks of age.

Orthotopic implantation of tumor cells and necropsy procedures. Hey A8, Hey A8 paclitaxel-resistant, and SKOV3ip1 cells were harvested from subconfluent cultures by a brief exposure to 0.25% trypsin and 0.02% EDTA. Trypsinization was stopped with medium containing 10% fetal bovine serum. The cells were then washed once in serum-free medium and resuspended in HBSS. Only single-cell suspensions with >95% viability, as determined by trypan blue exclusion, were used for the injections. To produce peritoneal tumors in mice, SKOV3ip1 and Hey A8 paclitaxel-resistant cells were injected i.p. in female nude mice at the concentration of 1×10^6 cells/0.2 mL HBSS; Hey A8 cells were injected i.p. at a concentration of 2.5×10^5 cells/0.2 mL HBSS. For different therapy experiments, mice were killed on days 29, 33, or 45. For survival experiments, mice were killed when moribund (unable to move or reach food). Tumors in the peritoneal cavity were excised and weighed. In animals bearing SKOV3ip1 tumors, malignant ascites was aspirated and measured. For immunohistochemistry and H&E staining procedures, tumors were fixed in formalin and embedded in paraffin. For immunohistochemistry requiring frozen tissue, tumors were embedded in optimum cutting temperature compound (Miles, Inc., Elkhart, IN), rapidly frozen in liquid nitrogen, and stored at −80°C.

Optimal treatment schedule and dose. To determine the optimal dose of AEE788, mice were injected i.p. with Hey A8 (2.5×10^5) or SKOV3ip1 (1.0×10^6) cells. Twenty-one days later, the nude mice were randomized into six groups (five mice per group): oral AEE788 given every other day at doses of 5, 12.5, 25, 50, and 100 mg/kg thrice and killed 4 hours after the last dose. Body weight, tumor weight, and ascites (for mice with SKOV3ip1 tumors) were recorded.

To determine the optimal treatment schedule, 21 days after the i.p. implantation of Hey A8 cells (2.5×10^5) or SKOV3ip1 cells (1×10^6), nude mice were randomized into three groups ($n = 8$): oral PBS or oral AEE788 at 25 or 50 mg/kg. The mice were treated orally every day for 3 days. Two mice per group were killed at 4, 24, 48, or 72 hours after the last oral treatment. Immunohistochemistry was done on the tumors as described below.

To determine the optimal dose of AEE788 and paclitaxel on established human ovarian carcinomas in the peritoneal cavity of nude mice, the mice were injected i.p. with SKOV3ip1 tumor cells. Seven days later, the mice were randomized into the following groups ($n = 10$): (*a*) oral PBS daily and i.p. once per week; (*b*) paclitaxel 75 μg i.p. once per week; (*c*) paclitaxel 125 μg i.p. once per week; (*d*) oral AEE788, 50 mg/kg, every other day; (*e*) oral AEE788, 100 mg/kg, every other day; (*f*) paclitaxel 75 μg i.p. once per week and oral AEE788, 50 mg/kg, every other day; (*g*) paclitaxel 75 μg i.p. once per week and oral AEE788, 100 mg/kg, every other day; (*h*) paclitaxel 125 μg i.p. once per week and oral AEE788, 50 mg/kg, every other day; and (*i*) paclitaxel 125 μg i.p. once per week and oral AEE788, 100 mg/kg, every other day. The mice were killed when moribund, and a survival analysis was done.

Therapy experiments. On the basis of our initial findings, we initiated a series of three separate therapy experiments and three survival experiments. Seven days after the i.p. injection of ovarian cancer cells, female nude mice were randomized into four groups (n = 10-12): (*a*) daily oral PBS and once per week PBS i.p.; (*b*) 125 μg i.p. paclitaxel once per week for SKOV3ip1 or Hey A8 paclitaxel-resistant cells or 100 μg i.p. paclitaxel once per week for Hey A8 cells; (*c*) AEE788 50 mg/kg every other day; and (*d*) 125 μg i.p. paclitaxel once per week and oral AEE788, 50 mg/kg, every other day for SKOV3ip1 or Hey A8 paclitaxel-resistant cells or 100 μg i.p. paclitaxel once per week and oral AEE788, 50 mg/kg, every other day for Hey A8 cells.

Immunohistochemistry. Paraffin sections (4 μm thick) were mounted on positively charged Superfrost slides (Fisher Scientific, Co., Houston, TX) and dried overnight. Immunohistochemical staining was done for the following antibodies: VEGFR (1:400 dilution), p-VEGFR (1:800 dilution), EGFR (1:400 dilution), and p-EGFR (1:100 dilution) at 4°C as previously described (27). Control samples were exposed to secondary antibody alone showed no nonspecific staining. For p-Akt staining, fresh frozen tissues were cut into 8 μm sections and mounted on positively charged slides. Sections were stored at −80°C. Immunohistochemistry with rabbit anti-mouse, human, rat (1:400 dilution) at 4°C was done.

Expression of PCNA and TUNEL was determined by immunohistochemistry using paraffin-embedded tissues (4-5 μm thick). Sections were deparaffinized in xylene, using a graded series of alcohol [100%, 95%, 80% ethanol/double-distilled water (v/v)], and rehydrated in PBS (pH 7.5). For PCNA immunohistochemistry, antigen retrieval was done by placing slides in distilled water and boiling in a microwave on high power for 5 minutes. Immunohistochemistry analysis of apoptotic cells was done using a commercially available TUNEL kit with modifications. Detection of PCNA, TUNEL, and CD31 was carried out as described previously (29).

Double immunofluorescence staining for CD31, and vascular endothelial growth factor receptor, epidermal growth factor receptor, or their phosphorylated forms. Fresh frozen ovarian tumors were cut into 8 μm sections and mounted on positively charged slides. Sections were fixed in cold acetone for 10 minutes, followed by washes with PBS. Slides were blocked with PBS supplemented with 4% cold water fish skin gelatin. Samples were then incubated overnight with rat anti-mouse CD31 (1:600 dilution) at 4°C. The slides were rinsed with PBS, incubated with protein blocking solution, and then incubated with goat anti-rat Alexa 594 (1:600 dilution) for 1 hour at room temperature. Next, all slides were rinsed thrice with PBS, incubated in protein blocking solution, and then incubated with a VEGFR, p-VEGFR, EGFR, or p-EGFR primary antibody overnight at 4°C (1:400, 1:600, 1:200, or 1:100 dilution, respectively). The slides were incubated with the corresponding fluorescent secondary antibody goat anti-rabbit Alexa 488 for 1 hour at room temperature (1:600 dilution). After PBS washes, Hoechst nuclear counterstain was applied.

Immunofluorescence double staining for CD31 and terminal deoxynucleotidyl transferase-mediated nick end labeling. Frozen tissues were used for CD31/TUNEL immunofluorescence double staining as described previously (30). Endothelial cells were identified by red fluorescence, and DNA fragmentation was detected by localized green fluorescence within the nucleus of apoptotic cells. Endothelial cells undergoing apoptosis were identified by yellow fluorescence (30).

Quantification of microvessel density, proliferating cell nuclear antigen, and terminal deoxynucleotidyl transferase-mediated nick end labeling. To quantify microvessel density, 10 random 0.159 mm^2 fields at ×100 magnification were examined for each tumor, and the microvessels within those fields were counted. A single microvessel was defined as a discrete cluster of cells stained CD31(+) and the presence of a lumen was required for scoring as a microvessel. For quantification of PCNA expression or TUNEL, the number of positive cells was quantified in 10 random 0.159 mm^2 at ×100 magnification.

Microscopy was done using a Nikon Microphot-FXA microscope (Nikon, Inc., Garden City, NY), and images were captured using a cooled charge-coupled device Hamamatsu 5810 camera (Hamamatsu Corp., Bridgewater, NJ) and Optimas Image Analysis software (Media Cybernetics, Silver Spring, MD). Photomontages were prepared using Micrografx Picture Publisher (Corel, Inc., Dallas, TX) and Adobe Photoshop software (Adobe Systems, Inc., San Jose, CA).

Statistical analyses. Comparisons of mean tumor weight, volume of ascites, and body weight were analyzed by ANOVA and t-tests using SPSS (SPSS, Inc., Chicago, IL). For comparisons of mean microvessel density, PCNA, and $TUNEL^+$ cells, Student's t-tests were used. Kaplan-Meier survival plots were generated and comparisons between survival curves were made with the log-rank statistic. A P-value of <0.05 was considered statistically significant.

Results

Inhibition of vascular endothelial growth factor receptor and epidermal growth factor receptor phosphorylation in human ovarian cancer cells by AEE788. In the first set of experiments, we used Western blot analyses to show the expression of

VEGFR, EGFR, p-VEGFR, and p-EGFR by cultured SKOV3ip1 ovarian cancer, ovarian endothelial, and mesentery endothelial cells. Cultured Hey A8 ovarian cancer cells only expressed the EGFR and p-EGFR. Next, the SKOV3ip1 ovarian cancer cells were cultured in serum-free complete MEM for 24 hours and then incubated for 15 minutes with 40 ng/mL of EGF. The cells were then incubated with medium only or different concentrations of AEE788. The expression of VEGFR and EGFR was unaffected, but phosphorylation of the EGFR was inhibited by AEE788 at concentrations of 0.1 to 0.5 μmol/L (Fig. 1A). The phosphorylation of the VEGFR was inhibited by AEE788 at concentrations of 1.0 to 2.0 μmol/L (Fig. 1B). Next, we determined the dose of AEE788 required to inhibit phosphorylation of the VEGFR and EGFR in tumor cells growing *in vivo*. Human ovarian cancer cells were injected into the peritoneal cavity of mice. Three weeks later, groups of mice were treated orally every other day for 3 days with 0, 25, or 50 mg/kg AEE788. Two mice were killed at 4, 24, 48, and 72 hours after the third oral treatment. The expression of both VEGFR and EGFR in Hey A8 and SKOV3ip1 tumors was unaffected by AEE788. Treatment with AEE788 at either 25 of 50 mg/kg inhibited phosphorylation of VEGFR for up to 48 hours, and phosphorylation of EGFR was inhibited for up to 72 hours. Inhibition of ascites, however, required at least 50 mg/kg of AEE788.

Therapy of ovarian cancer growth in the peritoneal cavity of nude mice. To determine the optimal biological dose, we did preliminary experiments with a range of doses of AEE788 alone or in combination with paclitaxel. Mice were injected i.p. with SKOV3ip1 cells, and 7 days later, the mice were treated orally with AEE788 at either 50 or 100 mg/kg along with i.p. paclitaxel once per week at 75 or 125 μg, or the combination of the AEE788 plus paclitaxel. Mice were killed 1 month later and autopsied. The results (data not shown; formal therapy experiments are presented below) suggested that the optimal biological dose of AEE788 was 50 mg/kg, and the lowest effective dose for paclitaxel in this ovarian cancer model was 125 μg; these doses were used for subsequent experiments. There was no additional therapeutic benefit with AEE788 at doses above 50 mg/kg in these experiments. Furthermore, AEE788 100 mg/kg was associated with diarrhea in mice.

In the first set of therapy experiments, mice were injected with the SKOV3ip1 cells into the peritoneal cavity. Seven days later, we began therapy according to the following groups: (*a*) oral saline and i.p. saline (control), (*b*) oral AEE788, 50 mg/kg, every other day and once per week i.p. saline, (*c*) once per week i.p. injection of paclitaxel at 125 μg/dose and oral saline every other day, and (4) oral AEE788, 50 mg/kg, every other day and once weekly i.p. 125 μg paclitaxel (Table 1A). Therapy with either AEE788 or paclitaxel decreased tumor weight and ascites. Treatment with AEE788 in combination with paclitaxel reduced the incidence of tumor and was highly effective in reducing tumor weight ($P < 0.001$) and eliminating ascites. The volume of ascites in mice treated with single-agent AEE788, paclitaxel-alone, and the combination of AEE788 and paclitaxel groups was significantly lower compared with control ($P = 0.005$). Treatment with AEE788, paclitaxel, or the combination therapy did not affect body weight ($P = 0.11$). To confirm the results seen in the SKOV3ip1 cell line, Hey A8 cells were injected into

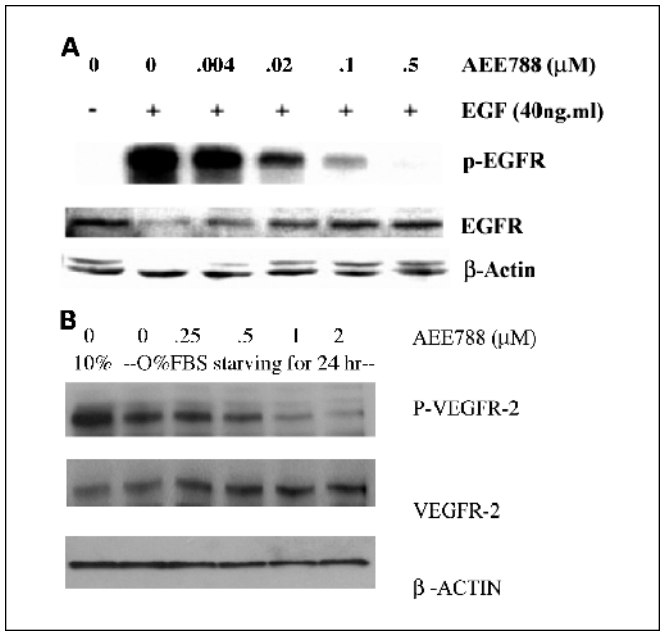

Fig. 1. *A,* expression of p-EGFR with varying concentrations of AEE788. Western analysis revealed that SKOV3ip1 express constitutive levels of EGFR in cell culture. In the absence of EGF (−) and in serum-free medium, EGFR remains in an unphosphorylated state. The addition of EGF (40 ng/mL) for 15 minutes to SKOV3ip1 stimulates EGFR activation. Phosphorylation of EGFR can be diminished by pretreating cells with increasing concentrations of AEE788. *B,* expression of p-VEGFR with varying concentrations of AEE788. Western analysis revealed that SKOV3ip1 express VEGFR, which is unaffected by increasing concentrations of AEE788. Phosphorylation of VEGFR can be inhibited by AEE788 concentrations of 1 to 2 μmol/L.

Table 1A. Therapy for SKOV3ip1 tumors in the peritoneal cavity of nude mice

Treatment group	Incidence*	Mean tumor weight ± SE (g)	*P*	Mean ascites (mL)	Mean body weight (g)
Control	10/12	0.99 ± 0.20		1.2	22.1 ± 0.8
AEE788	10/12	0.37† ± 0.11	<0.001	0.4	21.7 ± 0.6
Paclitaxel	11/12	0.16 ± 0.02	<0.001	0	23.1 ± 0.5
AEE788 ± paclitaxel	7/12	0.03†,‡ ± 0.01	<0.001	0‡	20.7 ± 0.9

NOTE: SKOV3ip1 cells (1×10^6 cells) were injected into the peritoneal cavity of female nude mice. Seven days later, treatment began; mice were necropsied on day 45. Tumor incidence, tumor weight, body weight, and ascites were determined.

*Number of mice with tumor/number of mice injected.

†$P < 0.001$ compared with paclitaxel.

‡$P = 0.005$ compared with AEE788 alone.

Table 1B. Therapy of Hey A8 tumors implanted orthotopically in nude mice

Treatment group	Incidence*	Mean tumor weight ± SE (g)	*P*	Mean body weight (g)
Control	10/12	1.84 ± 0.32		20.4 ± 0.7
AEE788	9/12	1.04 ± 0.26	0.06	20.5 ± 0.6
Paclitaxel	11/12	0.98† ± 0.18	0.02	20.8 ± 0.8
AEE788 ± paclitaxel	9/12	0.42‡ ± 0.15	0.002	21.2 ± 0.5

NOTE: Hey A8 cells (2.5×10^5) were injected into the peritoneal cavity of female nude mice. Seven days later, treatment began; mice were necropsied on day 29. Tumor incidence, tumor weight, and body weight were determined.
*Number of mice with tumor/number of mice injected.
† $P = 0.02$ compared with control.
‡ $P = 0.002$ compared with control or AEE788.

the peritoneal cavity of mice. Single-agent paclitaxel had therapeutic advantage over the saline control by reducing tumor weight by 47% (Table 1B). However, the AEE788-paclitaxel combination therapy was even more effective by reducing tumor weight by 77% ($P = 0.002$).

To determine whether the combination of AEE788 and paclitaxel was directed against the tumor cells that express activated receptors or also against the tumor-associated endothelial cells that express the activated EGFR and VEGFR, we conducted therapy experiments in nude mice implanted i.p. with the Hey A8 paclitaxel-resistant cells (Table 1C). As expected, in these mice, therapy with paclitaxel alone was ineffective. Single-agent AEE788 reduced the tumor weight compared with results for the control and paclitaxel treatment groups ($P = 0.001$). Mice given the combination therapy had further reduction in tumor weight compared with other treatment groups ($P < 0.001$). Thus, results in three different tumor cell lines show that combination therapy with AEE788 and paclitaxel decreases the progressive growth of human ovarian cancer in the peritoneal cavity of nude mice.

In the next set of experiments, we determined the effect of AEE788 alone or in combination with paclitaxel on survival of mice injected with SKOV3ip1 cells (Fig. 2A), Hey A8 cells (Fig. 2B), or paclitaxel-resistant Hey A8 cells (Fig. 2C) into the peritoneal cavity. For mice implanted with SKOV3ip1 or Hey A8 cells, single-agent AEE788 did not prolong survival; however, administration of paclitaxel resulted in prolonged survival. Combination of AEE788 and paclitaxel was even more effective in prolonging survival (Hey A8: median survival 34 days for controls versus 77 days for the combination group; SKOV3ip1: median survival 36 days for controls versus 78 days for the combination group. Both *P* values are <0.001). Administration of paclitaxel to mice implanted with paclitaxel-resistant Hey A8 cells did not improve survival (Fig. 2C), whereas single-agent AEE788 or AEE788 combined with paclitaxel significantly prolonged survival ($P < 0.001$).

Immunohistochemistry analysis. Immunohistochemistry analysis of SKOV3ip1, Hey A8, and Hey A8 paclitaxel-resistant tumors showed that tumor-associated endothelial cells expressed VEGFR, p-VEGFR, EGFR, and p-EGFR. Representative data for HeyA8 paclitaxel-resistant tumors are shown in Fig. 3 because the other two cell lines had similar results. Expression levels of VEGFR and EGFR were not reduced by any of the treatments. Endothelial cells in the HeyA8 paclitaxel-resistant tumors express VEGFR and EGFR (yellow fluorescence). Tumor cells and tumor-associated endothelial cells express both p-VEGFR and p-EGFR in mice treated with saline or only paclitaxel. In mice treated with AEE788 alone or with AEE788 and paclitaxel, the expression of p-VEGFR and p-EGFR by tumor cells and endothelial cells was decreased.

To further elucidate downstream effects of AEE788 on a key survival factor, immunohistochemistry analysis of paclitaxel-sensitive and paclitaxel-resistant tumors for the expression of phosphorylated Akt was done (Fig. 4). Treatment of mice with AEE788 alone or in combination with paclitaxel inhibits Akt phosphorylation, which may contribute to cell death. Next, the TUNEL method was used to evaluate tumor cell and tumor-associated endothelial cell apoptosis. When the double-labeled fluorescence technique is used, cells undergoing apoptosis (i.e., $TUNEL^+$ cells) exhibit green fluorescence, and endothelial

Table 1C. Therapy for Hey A8 paclitaxel-resistant tumors implanted orthotopically in nude mice

Treatment group	Incidence*	Mean tumor weight ± SE (g)	*P*	Mean body weight (g)
Control	10/10	2.27 ± 0.14		22.1 ± 0.9
AEE788	9/10	0.84 ± 0.19	0.001	22.6 ± 0.6
Paclitaxel	10/10	2.11 ± 0.13	0.42	22.4 ± 0.8
AEE788 ± paclitaxel	7/10	0.33†,‡ ± 0.09	<0.001	21.4 ± 0.9

NOTE: Hey A8 paclitaxel-resistant cells (1.0×10^6) were injected into the peritoneal cavity of female nude mice. Seven days later, treatment began; mice were necropsied on day 33. Tumor incidence, tumor weight, and body weight were determined.
*Number of mice with tumor/number of mice injected.
† $P = 0.03$ compared with AEE788 alone.
‡ $P < 0.001$ compared with control or paclitaxel.

cells ($CD31^+$) stain red (data summarized in Tables 2A and 2B). If there is colocalization, apoptotic endothelial cells have yellow nuclei. Data from experiments using SKOV3ip1 and Hey A8 paclitaxel-sensitive cells were pooled in Table 2A. In experiments using the paclitaxel-sensitive SKOV3ip1 and Hey A8 cells, minimal tumor cell or endothelial cell apoptosis was apparent in tumors from either control or single-agent AEE788 treatment groups (Table 2A). However, treatment with a combination of AEE788 and paclitaxel significantly increased the number of $TUNEL^+$ tumor cells from 6 ± 3 in the control group to 193 ± 62 ($P < 0.001$). Hey A8 paclitaxel-resistant tumors from mice treated with only saline, single-agent AEE788, or only paclitaxel did not exhibit much apoptosis of tumor cells (Table 2B). However, the combination therapy significantly increased the number of $TUNEL^+$ tumor cells from 4 ± 2 in the control group to 138 ± 65 ($P < 0.001$) in the paclitaxel-resistant tumors, suggesting that the combination therapy can inhibit progressive growth of tumors in part by an antivascular mechanism (data not shown).

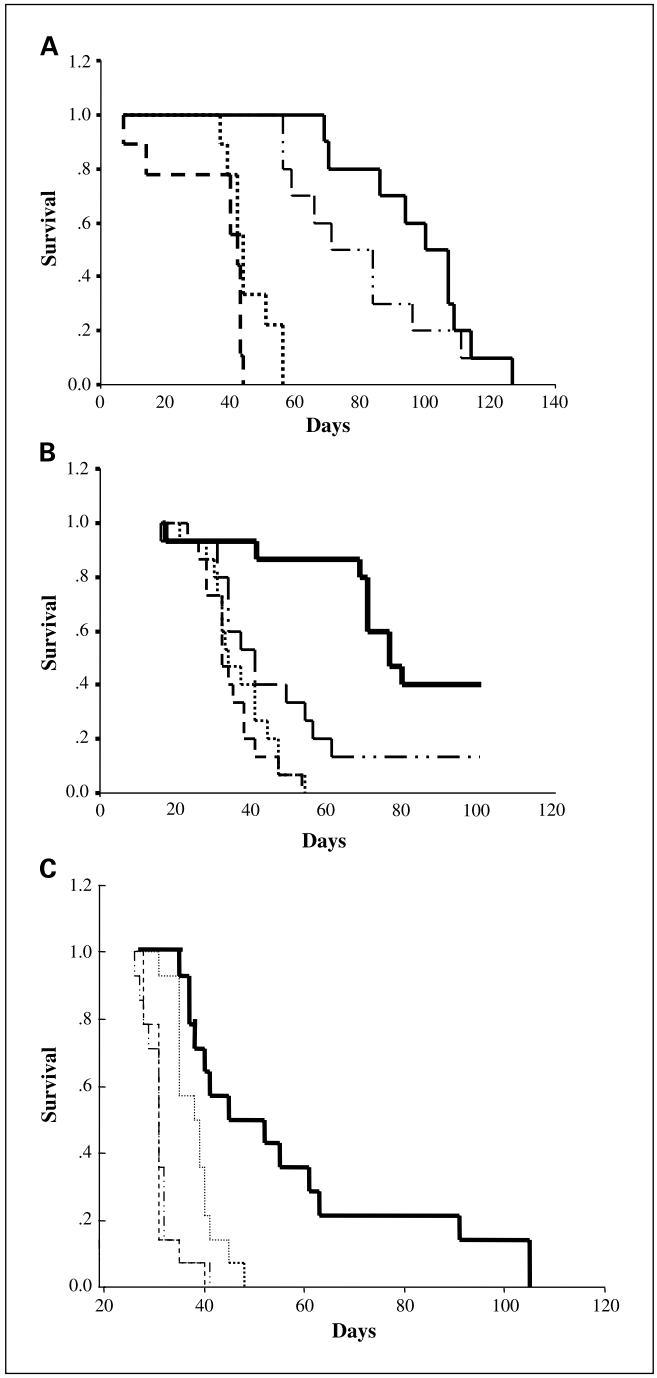

Fig. 2. *A,* Kaplan-Meier survival of SKOV3ip1 orthotopically injected mice based on therapy. Mice that received the combination therapy of 50 mg/kg AEE788 and 125 μg paclitaxel had the best survival compared with all other groups ($P < 0.001$). Control (- - -); AEE788 (. . . . . .); paclitaxel (-..-); combination (——). *B,* Kaplan-Meier survival of Hey A8 orthotopically injected mice based on therapy. Mice that received the combination therapy of 50 mg/kg AEE788 and 100 μg paclitaxel had the best survival compared with all other groups ($P < 0.001$). *C,* Kaplan-Meier survival of Hey A8 paclitaxel-resistant orthotopically injected mice based on therapy. Mice that received the combination therapy of 50 mg/kg AEE788 and 125 μg paclitaxel had the best survival compared with all other groups ($P < 0.001$). All groups had 10 mice. The equality of survival curves was tested using the log-rank statistic.

To further define the mechanism of action, we did immunohistochemistry for CD31 and PCNA to examine changes in microvessel density and proliferation, respectively (Fig. 5). Microvessel density was similar in the control and paclitaxel-treated tumors (22 ± 4 and 23 ± 5, respectively). Treatment with AEE788 alone or AEE788 with paclitaxel significantly decreased the microvessel density to 9 ± 2 ($P < 0.001$ versus control and paclitaxel alone groups; Table 2A). Similarly, PCNA was most significantly reduced in tumors receiving both paclitaxel and AEE788 ($P < 0.001$ versus all other groups). Hey A8 paclitaxel-resistant tumors from mice treated with only paclitaxel had no change in PCNA compared with either the control or single-agent AEE788 (Table 2B). However, tumors from mice treated with AEE788 and paclitaxel had a statistically significant decrease in PCNA (88 ± 28; $P < 0.001$ compared with controls). Similar to the paclitaxel-sensitive cell lines, microvessel density was similar in tumors from control and paclitaxel-treated mice (21 ± 13 in control; 21 ± 9 in paclitaxel). Tumors from mice treated with AEE788 and paclitaxel had significant reduction in microvessel density (4 ± 5; $P < 0.01$ compared with control and paclitaxel; $P = 0.01$ compared with single-agent AEE788). The combination therapy also induced necrosis in these tumors.

Discussion

Previously, it has been shown that expression of proangiogenic molecules, such as VEGF, by tumor cells can be stimulated by EGF signaling (31). Indeed, antiangiogenic effects, such as decreased tumor cell production of proangiogenic molecules and inhibition of tumor-associated angiogenesis, have been described for several ErbB family inhibitors (30). Therefore, our hypothesis was that the additional inhibition of VEGFR would not only act to accentuate the antitumor effects of EGFR inhibitors, but more importantly achieve antivascular therapy.

Blockade of the VEGFR and EGFR signaling pathways by oral administration of AEE788 combined with i.p. administration of paclitaxel significantly inhibited growth of paclitaxel-sensitive (SKOV3ip1 and Hey A8) and paclitaxel-resistant (Hey A8 paclitaxel-resistant) human ovarian cancer cells implanted into the peritoneal cavity of female nude mice. Paclitaxel reduced tumor weight by 46% to 83% in the paclitaxel-sensitive cell lines but not in the paclitaxel-resistant cell line. The oral administration of AEE788 alone reduced tumor growth in the paclitaxel-sensitive cell lines by 43% to 62% and in the

paclitaxel-resistant cell line by 70%. The combination of AEE788 and paclitaxel had the greatest effect in decreasing tumor weight and increased survival of mice inoculated with paclitaxel-sensitive or paclitaxel-resistant ovarian cancer cells.

In all ovarian tumors, VEGFR, p-VEGFR, EGFR, and p-EGFR were expressed by tumor cells and tumor-associated endothelial cells, suggesting that blockade of receptor activation could affect endothelial cells as well as tumor cells. Indeed, administration of paclitaxel produced apoptosis of paclitaxel-sensitive tumor cells but not paclitaxel-resistant tumor cells. However, treatment with both AEE788 and paclitaxel produced apoptosis in both tumor-associated endothelial cells and in tumor cells regardless of whether the tumors were resistant or sensitive to paclitaxel. These data, as well as previous data published from our laboratory (27), suggest that inhibition of receptor tyrosine kinase on endothelial cells coupled with the administration of anticycling drugs can produce apoptosis in tumor-associated endothelial cells. Endothelial cell death results in disruption of existing tumor-associated vasculature, leading to hypoxia, decreased cell proliferation, tumor cell apoptosis, and eventually necrosis. The destruction of tumor-associated endothelial cells with combination therapy of AEE788 and paclitaxel resulted in reducing tumor burden and prolonging survival (32).

Although AEE788 was effective in reducing tumor weight, the combination of AEE788 and paclitaxel was superior to the use of either agent alone. The inhibition of VEGFR and EGFR activation by AEE788 was not sufficient to induce the death of endothelial cells. However, the blockade of VEGFR and EGFR activation increased the sensitivity of tumor-associated endothelial cells to the effect of paclitaxel, suggesting that, in this orthotopic model, VEGF and EGF can function as survival or antiapoptotic factors (33–37). The finding that combination therapy was most effective against tumors produced by paclitaxel-resistant cells suggests that the primary target for therapy were the endothelial cells in the tumors and that their apoptosis led to a secondary wave of apoptosis in tumor cells. Collectively, these data suggest that the combination of AEE788 and paclitaxel reduces ovarian cancer growth by an antivascular mechanism. In contrast to cancer cells, tumor-associated endothelial cells are less likely to develop drug resistance (38). Moreover, unlike endothelial cells in normal tissues, endothelial cells in vasculature of neoplasms undergo frequent cell division (39, 40) and should, therefore, be sensitive to anticycling agents. Indeed, continuous, low-dose taxane-based therapy was found to be highly selective against cycling tumor-associated endothelial cells (41).

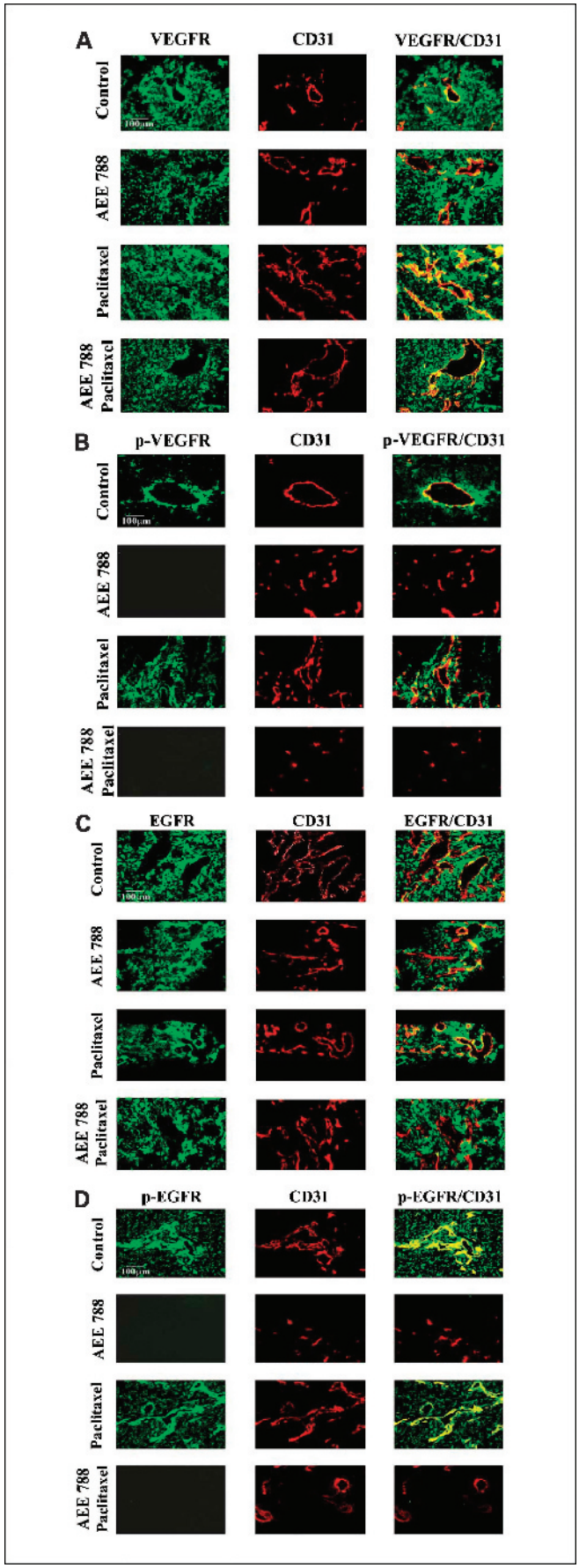

Fig. 3. Immunofluorescence double labeling of Hey A8 paclitaxel-resistant ovarian carcinoma cells growing in the peritoneal cavity of nude mice. Groups of mice were treated with saline, AEE788, paclitaxel, or AEE788 plus paclitaxel. Tumors were harvested on day 33 and processed for immunohistochemistry. Representative images of fluorescence immunohistochemistry are shown for VEGFR, CD31, and coexpression of CD31/VEGFR (*A*); and p-VEGFR, CD31, and coexpression of CD31/p-VEGFR (*B*). Representative images of fluorescence immunohistochemistry are shown for EGFR, CD31, and coexpression of CD31/EGFR (*C*); and p-EGFR, CD31, and coexpression of CD31/p-EGFR (*D*). Expression of VEGFR, EGFR, p-VEGFR, and p-EGFR is shown in green; CD31 expression is shown in red. Yellow indicates coexpression of CD31 and the receptor or phosphorylated receptor. Note that expression of VEGFR, EGFR, p-VEGFR, and p-EGFR was expressed by tumor-associated endothelial cells and that p-VEGFR and p-EGFR expression were down-regulated in groups of mice treated with AEE788 alone or in combination with paclitaxel. VEGFR and EGFR expression were not affected by therapy.

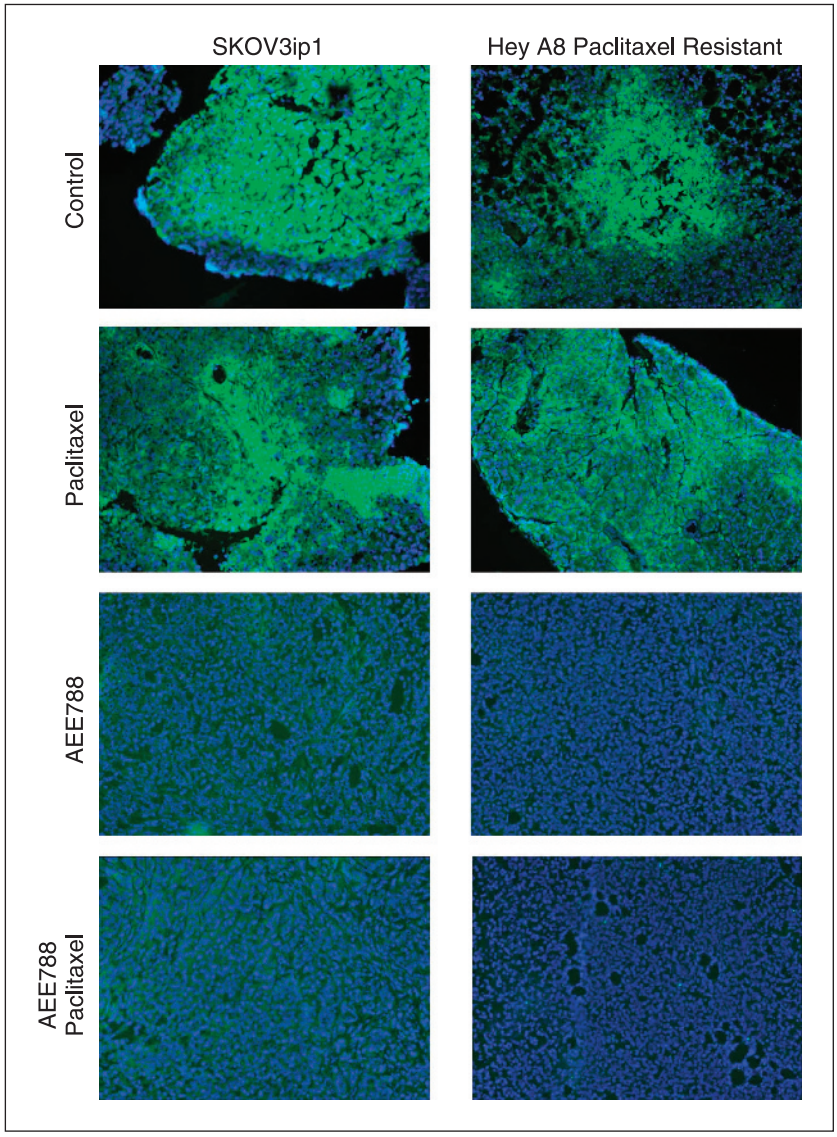

Fig. 4. p-Akt immunofluorescence of SKOV3ip1 and Hey A8 paclitaxel-resistant ovarian carcinoma cells growing in the peritoneal cavity of nude mice. Groups of mice were treated with saline, AEE788, paclitaxel, or AEE788 plus paclitaxel. Tumors were harvested on day 45 from SKOV3ip1-injected mice and on day 33 from Hey A8 paclitaxel-resistant–injected mice and processed for immunohistochemistry. Representative images of fluorescence immunohistochemistry are shown for p-Akt. The nuclei stain blue, whereas p-Akt stains green. Note that expression of p-Akt is decreased in the groups of mice that received AEE788 alone or in combination with paclitaxel.

Tissues regulate vascular architecture by signaling to endothelial cells through potent angiogenic agents such as VEGF. In particular, VEGF proteins modulate a range of endothelial cell behavior ranging from their initial patterning in the embryo, to their recruitment during wound healing or tumor angiogenesis, to their maintenance in normal tissues (42). It is important to note that VEGFRs are present on endothelial cells and nonendothelial cells such as ovarian tumor cells (43).

Table 2A. Immunohistochemical analysis of paclitaxel-sensitive human ovarian cancer tumors

Treatment group	Mean ± SD		
	CD31$^+$	PCNA$^+$	TUNEL$^+$
Control	22 ± 4	115 ± 31	6 ± 3
AEE788	9 ± 2*	80 ± 26	7 ± 4
Paclitaxel	23 ± 5	93 ± 22	22 ± 14†
AEE788 + paclitaxel	9 ± 2*	55 ± 25‡	193 ± 62‡

*$P < 0.001$ compared with control and paclitaxel.
†$P = 0.001$ compared with control and AEE788.
‡$P < 0.001$ compared with control, AEE788, and paclitaxel.

Table 2B. Immunohistochemical analysis of Hey A8 paclitaxel-resistant human ovarian tumors

Treatment group	Mean ± SD		
	CD31$^+$	PCNA$^+$	TUNEL$^+$
Control	21 ± 13	170 ± 35	4 ± 2
AEE788	10 ± 8*	147 ± 29	6 ± 4
Paclitaxel	21 ± 9	139 ± 18	5 ± 4
AEE788 ± paclitaxel	4 ± 5*	88 ± 28†	138 ± 65†

*$P < 0.01$ compared with control.
†$P < 0.001$ compared with control.

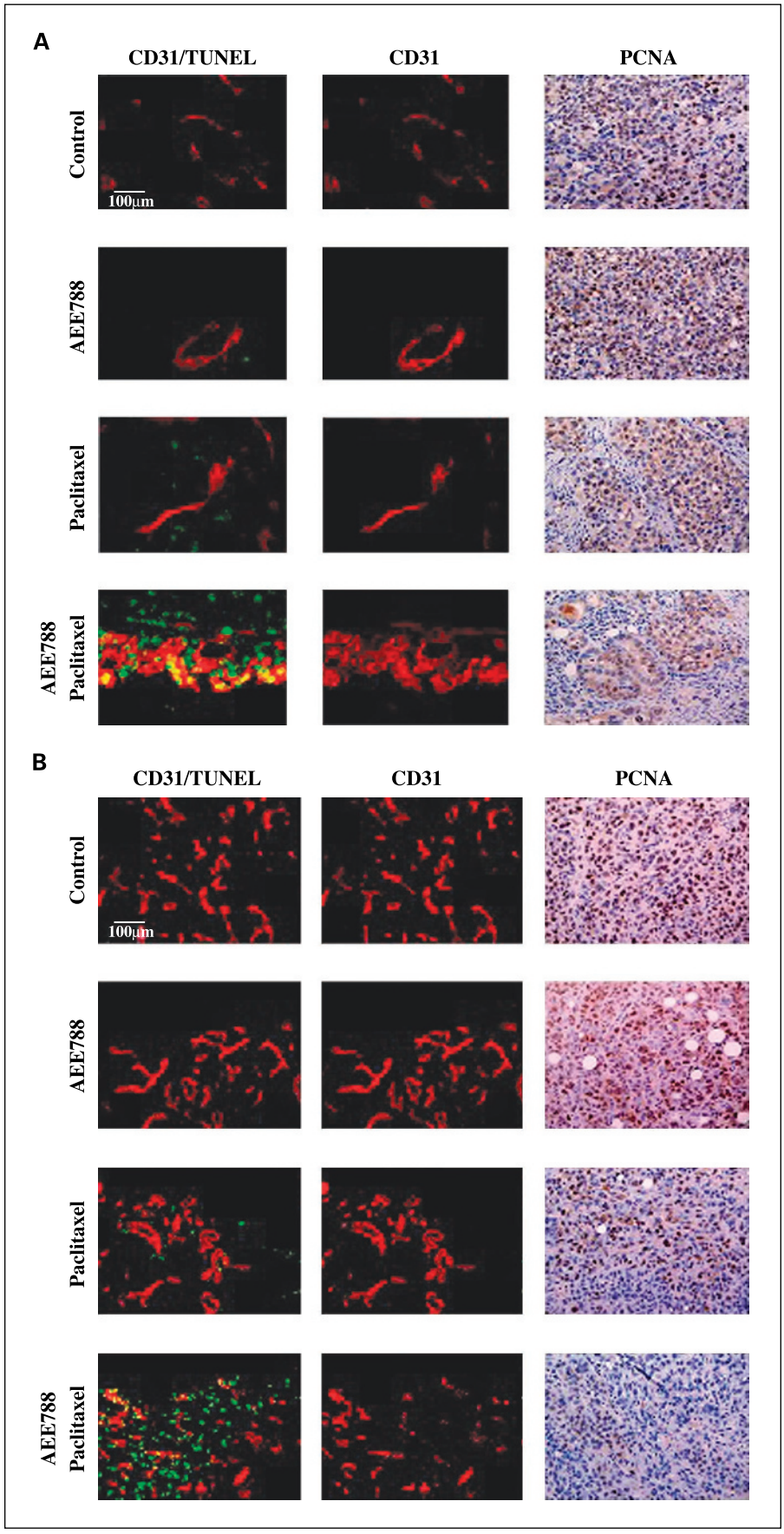

Fig. 5. Immunofluorescence and immunohistochemistry of tumors derived from the paclitaxel-sensitive cell line SKOVip1 (*A*) and HeyA8 paclitaxel-resistant human ovarian carcinoma (*B*) growing in the peritoneal cavity of nude mice. Groups of mice were treated with saline, AEE788, paclitaxel, or AEE788 plus paclitaxel. Tumors were harvested on day 45 or 33 and processed for immunohistochemistry. In the first column, representative images of fluorescence immunohistochemistry show $CD31^+$ cells (*red*) and tumor cells undergoing apoptosis (*green*). Yellow indicates a $CD31^+$ cell that has undergone apoptosis. The second column shows representative images of fluorescence immunohistochemistry for CD31, and the third column shows representative results of colorimetric immunohistochemistry analysis for PCNA (*brown*) for each treatment group. Note the reduction in microvessel density and $PCNA^+$ cells as well as increased necrosis caused by AEE788 and paclitaxel combination therapy.

EGF-mediated tumor angiogenesis has been shown previously. Angiogenesis in tumors secreting large amounts of transforming growth factor-α or EGF is associated with endothelial cells that express EGFR. The blockade of EGFR targets these vascular endothelial cells in the tumor tissue and ultimately result in cell death (28, 29). Additionally, monoclonal antibodies to EGFR inhibit tumor growth more potently in *in vivo* model systems than in *in vitro* cell culture studies, suggesting that mechanisms other than antiproliferative cell cycle effects must be contributing to tumor growth inhibition (44). VEGF and EGF are principal survival factors that inhibit apoptosis and proliferation by activation of the Ras/PI3-K/Akt pathway (34, 36). Akt can counteract apoptotic signaling by phosphorylating and inactivating caspase-9, proapoptotic protein Bad, and Forkhead transcription factors involved in the expression of proapoptotic proteins (45). VEGF protects endothelial cells against tumor necrosis factor-α and serum starvation–induced apoptosis (34, 46). Additionally, VEGF induces the expression of antiapoptotic proteins Bcl-2 and survivin in human endothelial cells (33–35). AEE788 inhibits phosphorylation of EGFR and VEGFR and consequently reduces activation of mitogen-activated protein kinase, Akt, and phosphoinositide-3 kinase. The endothelial cells and tumor cells are then vulnerable to cytotoxic agents such as paclitaxel. These data confirm the potential role of VEGF and EGF as survival factors.

Other mechanisms may explain the additive effects of AEE788 and paclitaxel in addition to their effects on VEGF, VEGFR, EGF, and EGFR. Inhibition of VEGFR signaling in tumor stroma can increase tumor uptake of chemotherapeutic agents, occurring most likely as a consequence of decreased tumor interstitial fluid pressure by producing a morphologically and functionally "normalized" vascular network and not by restoring lymphatic function (47). The exact mechanism by which inhibition of EGFR signaling causes chemosensitization, however, remains controversial (44). Blockade of EGFR causes an inhibition of cyclin-dependent kinase-2 and cell cycle arrest in the G_1 phase (44). Additionally, it is well established that paclitaxel exerts its cytotoxic effects by binding α-tubulin and stabilizing microtubular structures, leading to cell cycle arrest (48). Therefore, combination of AEE8788 and paclitaxel may have additive effects by targeting cell cycle arrest.

Cancer is a heterogeneous disease that requires multimodality therapy (49). Although paclitaxel is an effective, well-tolerated first-line chemotherapeutic agent for treatment of ovarian cancer, many patients will develop paclitaxel-resistant tumors, and then treatment of the disease requires targeting host factors. Recently, bevacizumab (VEGF neutralizing monoclonal antibody), in combination with chemotherapy, resulted in improved progression-free and overall survival in advanced colorectal carcinoma, leading to its approval by the U.S. Food and Drug Administration for first-line treatment for patients with metastatic colorectal cancer (50). Based on encouraging results with antivascular targeting in other cancers and our preclinical data, it is possible that dual blockers of VEGFR and EGFR signaling, such as AEE788, in combination with chemotherapy may enhance survival of patients with advanced or recurrent ovarian carcinoma. AEE788 has recently entered phase I clinical trials in cancer patients; however, its combination with chemotherapy in clinical trials remains to be studied.

Acknowledgments

We thank Novartis Pharma for providing AEE788 and for critical discussion and support, and Michael Worley for critical editorial review and Lola López for expert preparation of this manuscript.

References

1. Jemal A, Tiwari RC, Murray T, et al. Cancer statistics, 2004. CA Cancer J Clin 2004;54:8–29.
2. Cannistra SA. Cancer of the ovary. N Engl J Med 1993;329:1550–9.
3. du Bois A, Luck H, Meier W, et al. A randomized clinical trial of cisplatin/paclitaxel versus carboplatin/paclitaxel as first-line treatment of ovarian cancer. J Natl Cancer Inst 2003;9:1320–9.
4. McGuire WP, Hoskins WJ, Brady MF, et al. Cyclophosphamide and cisplatin compared with paclitaxel and cisplatin in patients with stage III and stage IV ovarian cancer. N Engl J Med 1996;334:1–6.
5. Bookman MA, McGuire WP, Kilpatrick D, et al. Carboplatin and paclitaxel in ovarian carcinoma: a phase I study of the Gynecologic Oncology Group. J Clin Oncol 1996;14:1895–902.
6. Gore ME. Treatment of relapsed epithelial ovarian cancer. In: American Society of Clinical Oncology 2001 education book. Alexandria (VA): American Society of Clinical Oncology; 2001. p. 468–76.
7. Folkman J. What is the evidence that tumors are angiogenesis dependent? J Natl Cancer Inst 1990; 82:4–6.
8. Robinson CJ, Stringer SE. The splice variants of vascular endothelial growth factor (VEGF) and their receptors. J Cell Sci 2001;114:853–65.
9. Shweiki D, Itin A, Soffer D, Keshet E. Vascular endothelial growth factor induced by hypoxia may mediate hypoxia-initiated angiogenesis. Nature 1992;359: 843–5.
10. Ferrara N, Alitalo K. Clinical applications of angiogenic growth factors and their inhibitors. Nat Med 1999; 5:1359–64.
11. Abu-Jawdeh GM, Faix JD, Niloff J, et al. Strong expression of vascular permeability factor (vascular endothelial growth factor) and its receptors in ovarian borderline and malignant neoplasms. Lab Invest 1996; 74:1105–15.
12. Paley PJ, Staskus KA, Gebhard K, et al. Vascular endothelial growth factor expression in early stage ovarian carcinoma. Cancer 1997;80:98–106.
13. Cooper BC, Ritchie JM, Broghammer CLW, et al. Preoperative serum vascular endothelial growth factor levels: significance in ovarian cancer. Clin Cancer Res 2002;8:3193–7.
14. Xu L, Yoneda J, Herrera C, Wood J, Killion JJ, Fidler IJ. Inhibition of malignant ascites and growth of human ovarian carcinoma by oral administration of a potent inhibitor of the vascular endothelial growth factor receptor tyrosine kinases. Int J Oncol 2000;16:445–54.
15. Morishige K, Kurachi H, Amemiya K, et al. Evidence for the involvement of transforming growth factor α and epidermal growth factor receptor autocrine growth mechanism in primary human ovarian cancers *in vitro*. Cancer Res 1991;51:5322–8.
16. Ottensmeier C, Swanson L, Strobel T, Druker B, Niloff J, Cannistra SA. Absence of constitutive EGF receptor activation in ovarian cancer cell lines. Br J Cancer 1996;74:446–52.
17. Bartlett JMS, Langdon SP, Simpson BJB, et al. The prognostic value of epidermal growth factor mRNA expression in primary ovarian cancer. Br J Cancer 1996; 73:301–6.
18. Baron AT, Lafky JM, Boardman CH, et al. Serum sErbB1 and epidermal growth factor levels as tumor biomarkers in women with stage III or IV epithelial ovarian cancer. Epidemiol Biomarkers Prev 1999; 8:129–37.
19. Huang LW, Garrett AP, Bell DA, Welch WR, Berkowitz RS, Mok SC. Differential expression of matrix metalloproteinase-9 and tissue inhibitor of metalloproteinase-1 protein and mRNA in epithelial ovarian tumors. Gynecol Oncol 2000;77:369–76.
20. Ellerbroek SM, Halbleib JM, Benavidez M, et al. Phosphatidylinositol 3-kinase activity in epidermal growth factor-stimulated metalloproteinase-9 production and cell surface association. Cancer Res 2001; 61:1855–61.
21. Berchuck A, Rodriguez GC, Kamel A, et al. Epidermal growth factor receptor in normal ovarian epithelium and ovarian cancer. Am J Obstet Gynecol 1991;164: 669–74.
22. Alper O, Bermann-Leitner ES, Bennett TA, Hacker NF, Stromberg K, Stetler-Stevenson WG. Epidermal growth factor receptor signaling and the invasive phenotype of ovarian carcinoma cells. J Natl Cancer Inst 2001;93:1375–84.
23. Traxler P, Allegrini PR, Brandt R, et al. AEE788: A dual family epidermal growth factor receptor/ErbB2 and vascular endothelial growth factor receptor tyrosine kinase inhibitor with antitumor and antiangiogenic activity. Cancer Res 2004;64:4931–41.
24. Buick RN, Pullano R, Trent JM. Comparative properties of five human adenocarcinoma cell lines. Cancer Res 1985;45:3668–76.
25. Yu D, Wolf JK, Scanlon M, Price JE, Hung MC. Enhanced c-erbB-2/neu expression in human ovarian cancer cells correlates with more severe malignancy that can be suppressed by E1A. Cancer Res 1993; 53:891–8.
26. Yoneda J, Kuniyasu H, Crispens MA, Price JE, Bucana CD, Fidler IJ. Expression of angiogenesis-related

genes and progression of human ovarian carcinomas in nude mice. J Natl Cancer Inst 1998;90:447–54.

27. Apte SM, Fan D, Killion JJ, Fidler IJ. Targeting the platelet-derived growth factor receptor in antivascular therapy for human ovarian carcinoma. Clin Cancer Res 2004;10:897–908.

28. Langley RR, Ramirez KM, Tsan RZ, Van Arsdall M, Nilsson MB, Fidler IJ. Tissue-specific microvascular endothelial cell lines from *H-2K^b-ts* A58 mice for studies of angiogenesis and metastasis. Cancer Res 2003;63:2971–6.

29. Kim SJ, Uehara H, KarashimaT, Shepherd DL, Killion JJ, Fidler IJ. Blockade of epidermal growth factor signaling in tumor cells and tumor-associated endothelial cells for therapy of androgen-independent human prostate cancer growing in the bone of nude mice. Clin Cancer Res 2003;9:1200–10.

30. Baker CH, Kedar D, McCarty MF, et al. Blockade of epidermal growth factor receptor signaling on tumor cells and tumor-associated endothelial cells for therapy of human carcinomas. Am J Pathol 2002;161:929–38.

31. Maity A, Pore N, Lee J, Solomon D, O'Rourke DM. Epidermal growth factor receptor transcriptionally up-regulates vascular endothelial growth factor expression in human glioblastoma cells via a pathway involving phosphatidlyinositol 3′-kinase and distinct from that induced by hypoxia. Cancer Res 2000; 60:5879–86.

32. Klement G, Baruchel S, Rak J, et al. Continuous low-dose therapy with vinblastine and VEGF receptor-2 antibody induces sustained tumor regression without overt toxicity. J Clin Invest 2000;105:R15–24.

33. Gerber HP, Dixit V, Ferrara N. Vascular endothelial growth factor induces expression of the antiapoptotic proteins Bcl-2 and A1 in vascular endothelial cells. J Biol Chem 1998;273:13313–6.

34. Gerber HP, McMurtrey A, Kowalski J, et al. Vascular endothelial growth factor regulates endothelial cell survival through the phosphatidylinositol 3′ kinase/Akt signal transduction pathway. Requirement for Flk-1/KDR activation. J Biol Chem 1998; 273:30336–43.

35. Tran J, Rak J, Sheehan C, et al. Marked induction of the IAP family antiapoptotic proteins surviving and XIAP by VEGF in vascular endothelial cells. Biochem Biophys Res Commun 1999;264:781–8.

36. Datta SR, Dudek H,Tao X, et al. Akt phosphorylation of BAD couples survival signals to the cell-intrinsic death machinery. Cell 1997;91:231–41.

37. Shimamura A, Ballif BA, Richards SA, Blenis J. Rsk1 mediates a MEK-MAP kinase cell survival signal. Curr Biol 2000;10:127–35.

38. Fidler IJ. The organ microenvironment and cancer metastasis (Review). Differentiation 2002;70: 498–505.

39. Hobson B, Denekamp J. Endothelial proliferation in tumours and normal tissues: continuous labeling studies. Br J Cancer 1984;49:405–13.

40. Eberhard A, Kahlert S, Goede V, Hemmerlein B, Plate KH, Augustin HG. Heterogeneity of angiogenesis and blood vessel maturation in human tumors: implications for antiangiogenic tumor therapies. Cancer Res 2000;60:1388–93.

41. Bocci G, Nicolson KC, Kerbel RS. Protracted low-dose effects on human endothelial cell proliferation and survival *in vitro* reveal a selective antiangiogenic window for various chemotherapeutic drugs. Cancer Res 2002;62:6938–43.

42. Ferrara N, Alitalo K. Clinical applications of angiogenic growth factors and their inhibitors. Nat Med 1999;5:1359–64.

43. Boocock CA, Charnock-Jones S, Sharkey AM, et al. Expression of vascular endothelial growth factor and its receptors flt and KDR in ovarian carcinoma. J Natl Cancer Inst 1995;87:506–16.

44. Mendelsohn J. Targeting the epidermal growth factor receptor for cancer therapy—David A. Karnofsky Award Lecture. J Clin Oncol 2002;18:1–13s.

45. Datta SR, Brunet A, Greenberg ME. Cellular survival: a play in three Akts. Genes Dev 1999;13:2905–27.

46. Spyridopoulos I, Brogi E, Kearney M, et al. Vascular endothelial growth factor inhibits endothelial cell apoptosis induced by tumor necrosis factor-α: balance between growth and death signals. J Mol Cell Cardiol 1997;29:1321–30.

47. Tong RT, Boucher Y, Kozin SV, Winkler F, Hicklin DJ, Jain RK. Vascular normalization by vascular endothelial growth factor receptor 2 blockade induces a pressure gradient across the vasculature and improves drug penetration in tumors. Cancer Res 2004;64:3731–6.

48. Jordan MA, Toso RJ, Thrower D, Wilson L. Mechanism of mitotic blockade and inhibition of cell proliferation by Taxol at low concentrations. Proc Natl Acad Sci U S A 1993;90:9552–6.

49. Fidler IJ. The pathogenesis of cancer metastasis: the "seed and soil" hypothesis revisited (Timeline). Nat Rev Cancer 2003;9:453–8.

50. Hurwitz H, Fehrenbacher L, Novotny W, et al. Bevacizumab plus irinotecan, fluorouracil, and leucovorin for metastatic colorectal cancer. N Engl J Med 2004; 350:2335–42.